Hydrophobisation of activated carbon fiber and the influence on the adsorption selectivity towards carbon disulfide

Zunyuan Xie [a,b], Feng Wang [a], Ning Zhao [a], Wei Wei [a,*], Yuhan Sun [a,c,**]

[a] State Key Laboratory of Coal Conversion, Institute of Coal Chemistry, Chinese Academy of Sciences, Taiyuan, 030001, PR China
[b] Graduate School of Chinese Academy of Sciences, Beijing, 100049, PR China
[c] Low Carbon Conversion Center, Shanghai Advanced Research Institute, Chinese Academy of Sciences, Shanghai, 201203, PR China

ARTICLE INFO

ABSTRACT

The hydrophobisation of commercial viscose-based activated carbon fiber (ACF) was obtained by grafting vinyltrimethoxysilane (vtmos) on the ACF surface, to improve ACF's adsorption selectivity towards carbon disulfide (CS_2) under highly humid condition. The characterizations, including FTIR, ^{29}Si NMR, adsorption/desorption of nitrogen, thermal analysis and elemental analysis, revealed that the vtmos was successfully grafted onto the ACF surface, even though the hydrophobisation caused a partial filling of the porosity along with a slight decrease in the surface area. The efficiency of the hydrophobisation modification was evaluated by both equilibrium and dynamic adsorption experiment of water vapor and CS_2. The equilibrium adsorption results indicated that the hydrophobisation modifications accounted for a decrease of both the amounts of water and CS_2 adsorbed by the hydrophobised ACF. However, dynamic adsorption found that the adsorption performance was improved under highly humid condition, evidencing that hydrophobisation improved the hydrophobicity of the ACF surface and enhanced the adsorption selectivity towards CS_2.

© 2010 Published by Elsevier B.V.

1. Introduction

Carbon disulfide (CS_2) is one of the sulfur-containing compounds existing in natural gas, petroleum and various raw gases from coal. Since CS_2 possesses high toxicity with a maximum permissible concentration in air of $0.5 \, mg/m^3$, its emission into atmosphere even in small amounts is inadmissible, which triggers an increasing interest in finding reliable, cost effective technologies for its control [1–3]. There are several approaches to remove CS_2 from the off-gas [4–8]. Among them, adsorption process is widely investigated for the removal of CS_2 because of its simplicity and effectiveness [2,9–13]. Currently, one of the keys in adsorption process is the adsorbents with high performance in both equilibrium and kinetics.

Amongst all the presented adsorbents in the adsorption process, activated carbon fiber (ACF) is recognized to be one of the most promising adsorbents due to its high BET surface area, large pore volume, and uniform microporosity, and then widely used for removal of various pollutants, especially for adsorption of volatile

organic compounds (VOCs) [14–19]. However, carbon-based materials have the self-defect that the adsorption property is greatly affected by the water vapor [20,21]. It was reported that the adsorption performance of ACF decreased greatly when the humidity was higher than 65% in the adsorption process of CS_2 [12]. Fan et al. [21] have investigated the performance of organic amine modified activated carbon for the adsorption of CS_2 with the influence of water vapor, which was greatly affected by water vapor due to the existence of oxygen-containing groups on the carbon surface which had a strong affinity to water and suppressed the uptake of adsorbates on the carbon surface.

In order to enhance the performance of ACF under the high humidity condition, it is necessary to improve the hydrophobicity of ACF and lower the affinity between oxygen-containing groups and water. For this purpose, some techniques were developed by removing the oxygen-containing groups of carbon-based materials via the surface modification [22–33]. Among them, the physical methods were conventionally used via thermal treatment in inert gas [23,24]. However, the texture was changed drastically due to the high temperature treatment. In contrast, the chemical methods were handled by chemical reactions (coating, impregnation and plasma treatment) with the slight change of the texture [25–28]. For instance, Budarin et al. and Cosnier et al. reported grafting vinyltrimethoxysilane (vtmos) organosilicon compounds onto the surface of activated carbon respectively [25,26]. This method was proved to be effective, only with the disadvantage of the slight

* Corresponding author.
Fax: +86 351 4041153.
** Corresponding author at: State Key Laboratory of Coal Conversion, Institute of Coal Chemistry, Chinese Academy of Sciences, Taiyuan, 030001, PR China.
Fax: +86 351 4041153.
E-mail addresses: weiwei@sxicc.ac.cn (W. Wei), yhsun@sxicc.ac.cn (Y. Sun).
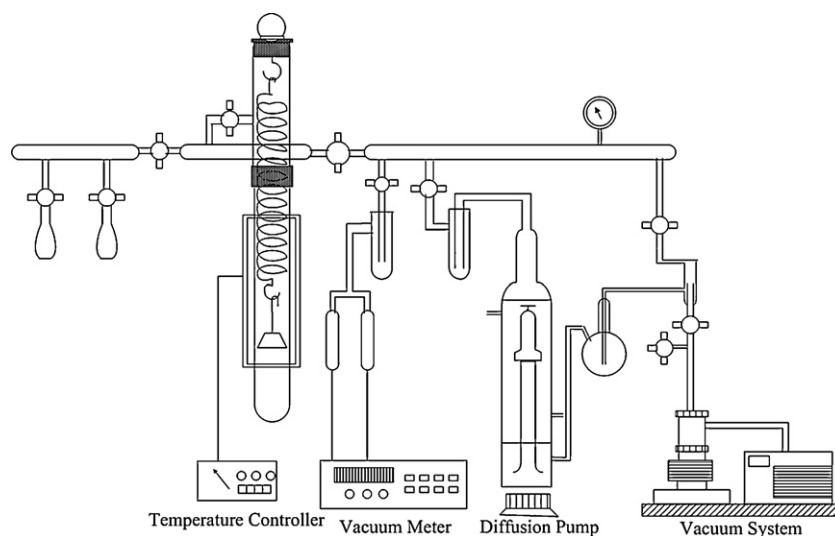
Fig. 1. Schematic setup of static adsorption.

reduction in the BET surface areas and pore volumes. Unfortunately, so far few hydrophobisation of ACF have been reported, especially with the chemical method. The hydrophobisation of viscose-based commercial ACF was therefore carried out by using vinyltrimethoxysilane (vtmos) as a hydrophobic agent to improve the adsorption selectivity towards carbon disulfide (CS_2) under highly humid condition in the present work.

2. Materials and methods

2.1. Materials

The commercial viscose-based ACF used for modification was obtained from Anshan Senxin Activated Carbon Fiber plant. The vtmos, used as hydrophobic agent, was from J&R Chemical Ltd. Sodium borohydride ($NaBH_4$) was produced by Sinopharm Chemical Reagent Co., Ltd. Hydrogen peroxide (H_2O_2), CS_2 and other chemicals were purchased from Tian Da chemical Company. All the chemicals used were analytical-reagent certified grade or better.

2.2. Pretreatment and hydrophobisation

The commercial ACF used in this work was first treated before hydrophobisation modification according to the literature [25,26]. The pretreatment increased the density of hydroxyl groups and limited the amount of other oxygen-containing groups. And then the organosilicon compound was grafted onto the ACF surface.

The experimental procedures for hydrophobisation modification in this work were conducted as the following steps. (1) Oxidation: 5 g ACF was first added to 500 ml of 15% H_2O_2 (w/w) [34] to produce acidic surface groups (mainly carboxylic acid, lactone and phenol groups). Then, the ACF was washed by water and dried at 100 °C. Afterwards, the ACF was heat-treated at 450 °C for 3 h under the protection of N_2 atmosphere, which remained hydroxyls, carbonyls and related functional groups and removed some other oxygen-containing groups [25,26]. The sample after this treatment was named as ACF-O. (2) Reduction: The ACF-O was treated by $NaBH_4$ solution dissolved in anhydrous methanol with the ratio 5 g: 500 ml. The ACF-O was submerged by the mixture for 12 h in the operation. Afterwards, 500 ml water was added to the mixture and boiled for 3 h. After that, the sample was separated from the mixture, washed by water and dried in the oven. The sample obtained after reduction treatment was named as ACF-R. (3) Hydrophobisation: The hydrophobisation modification of the ACF was carried out

after the aforementioned treatments. It was conducted by adding the ACF-R to the solution of organosilicon dissolved by toluene. And small amount of water was also added to the solution for inducing the hydrolysis of the alkoxysilane molecules. The condensation reaction was operated at 110 °C for hours. After the final procedures of treatment by soxhlet extraction with toluene for 3–6 h, the sample of the hydrophobised ACF was finally obtained, which was named as ACF-H.

2.3. Characterization

The vibration frequency changes of the functional groups on the ACF surface before and after hydrophobisation were determined by Fourier transform infrared spectroscopy. The results were recorded on a FTIR spectrometer NICOLET NEXUS 470FTIR (Thermo). 1 mg of ACF sample was mixed with 500 mg of potassium bromide (KBr), and the pellets were prepared by pressing the blend 10 min under 7 tons/cm². The solid-state NMR spectrum of ^{29}Si using magic angle spinning (MAS) at 300 MHz was conducted on an AVANCE III 400 Bruker spectrometer.

The pore structure parameters of the samples were based on the nitrogen adsorption isotherms, determined at 77 K with an ASAP 2020M apparatus. The micropore (V_{micro}) volume was calculated by t-plot method. The micropore width and micropore size distribution (MPSD) were calculated by BJH method. The stability of the covalently bound of the functional groups presented on ACF surface was investigated by thermal analysis using a TG/DTA 92–16.18 (Setaram). The heating rate was 2 K/min from 293 K to 1273 K under argon at a flow rate of 40 ml/min. The wetting properties of ACF and ACF-H were determined by a Dynamic Contact Angle Meter and Tensiometer apparatus (DCAT21, Dataphysics) based on the method of Washburn method. And the carbon, oxygen and the silicon contents were analyzed by X-ray photoelectron spectroscopy (XPS, ESCALAB250, Thermo).

2.4. Adsorption performance

The static adsorption was operated in a glass vacuum system shown in Fig. 1. The adsorption system was heated to a certain temperature under the vacuum of 10^{-2} Pa and kept for 2 h before adsorption taking place. The adsorption system was maintained at 293.15 K during the adsorption process. And the vapor, which produced from the liquid CS_2 and water stored inside the respective small vessels, was introduced to the adsorption device by discon-
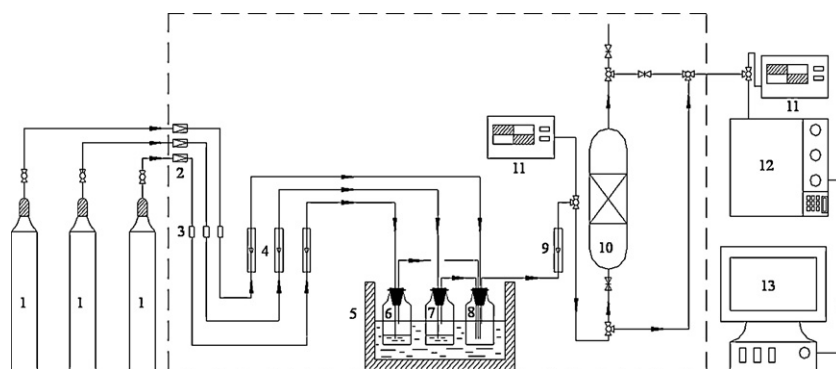
Fig. 2. Schematic setup of dynamic adsorption, (1) Nitrogen gas, (2) Pressure reducing value, (3) Stable-flow value, (4 and 9) Rotating flowmeter, (5) Constant temperature water bath, (6) Water vapor generator, (7) CS$_2$ generator, (8) Buffering bottle, (10) Adsorber, (11) Humidity and temperature sensor, (12) Gas chromatography, (13) Workstation.

tinuous introductions. About 100 mg of samples were packed in the small quartz basket in the glass vacuum system. The corresponding uptakes were thus measured point to point. The adsorption equilibrium was usually attained within 30 min.

The dynamic adsorption of CS$_2$ was carried out in the adsorption apparatus shown in Fig. 2. The gas-phase CS$_2$ and water vapor were generated by nitrogen-blowing method and then mixed and diluted to a certain concentration. The concentration of CS$_2$ was regulated and controlled at 0.32 mg/l with the relative humidity 70%. The flow rate of mixture gas through the adsorber bed was 0.3 l/min controlled by the flow-meter. The inner diameter of adsorber was 50 mm, and the density of the sample was about 0.045 g/cm^3. All the experiments were operated at the temperature of 303.15 K.

3. Results and discussion

3.1. Surface grafting

It is generally accepted that the hydrophobisation can form surface organosilicon-containing groups on the surface of the sample. In this study, FTIR spectroscopy and NMR spectra of ^{29}Si were used to characterize the chemical surface of the virgin and hydrophobised ACF.

The FTIR spectra of ACF and ACF-H are presented in Fig. 3. It could be observed that ACF-H showed the absorption bands at 2924, 2854, 1630, 1469, 1400 and 1100 cm^{-1}. The absorption bands at 2924, 2854 and 1469 cm^{-1}, which had not been observed from ACF, were assigned to asymmetric stretching, symmetric stretching and asymmetric deformation of CH$_3$ of Si–O–CH$_3$ respectively, and the absorption band at 1100 cm^{-1} was due to the stretching vibration of Si–O of Si–O–CH$_3$. These findings indicated the existence of
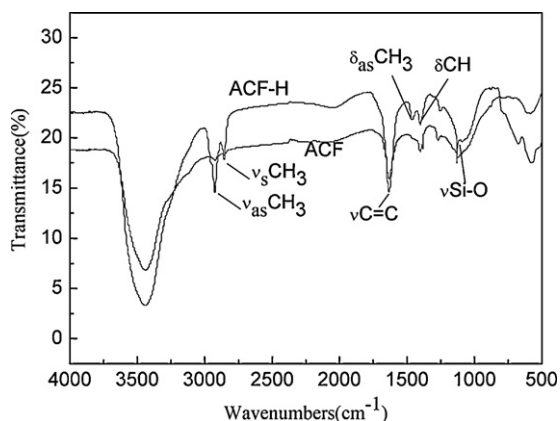
methoxysilyl structural unit corresponding to vtmos [37]. Moreover, the appearance of the bands at 1630 cm^{-1} and 1406 cm^{-1}, corresponding to C=C stretching vibration and CH deformation vibration in H$_2$C=CH– group, gave the further evidence of the existence of vtmos.

Simultaneously, the chemical shift for the absorption bands at 2924, 2854, 1630, 1469, 1400 and 1100 cm^{-1} were observed, which were different from those at 2945, 2843, 1600, 1458, 1411 and 1088 cm^{-1} in the standard spectrum of vtmos. Such a shift should be closely related to a possible variation of the rigidity of the molecule grafted on ACF surface. Additionally, the absorption band at 1194 cm^{-1} in the standard spectrum of vtmos which corresponded to the rocking vibrations of CH$_3$ in Si–O–CH$_3$ [37,38], was not found in the spectrum of ACF-H, further indicating that the variation of the molecule rigidity of vtmos. As a result, these findings illustrated that the vtmos was not simply adsorbed but grafted on the surface of ACF.

Moreover, the two characteristic absorption bands at 773 cm^{-1} and 817 cm^{-1}, which were attributed to the C–O stretching vibration of vtmos and the C–C–C in-plane bending ascribed to the polymer of vtmos respectively, were not found in the spectrum of ACF-H. These findings gave the further evidence that the vtmos was not simply adsorbed on the surface of ACF [26,38]. The disappearance of the absorption band at 773 cm^{-1}, meaning the decrease of Si–O–CH$_3$ group, supported the hypotheses that the hydrophobisation took place by condensation reaction between Si–O–CH$_3$ group and the –C–OH group on ACF surface. Meanwhile, the reaction probability of polymerization between vtmos was decreased by the grafting of vtmos on ACF surface. That explained the disappearance of the absorption band at 817 cm^{-1}. In summary, these results illustrated by the IR spectra of ACF and ACF-H suggested that hydrophobisation was achieved by grafting the functional groups of vtmos on ACF surface rather than adsorbing on ACF.

Besides, the existence of the absorption bands (2924, 2854 and 1469 cm^{-1}) due to the vibration of CH$_3$ of Si–O–CH$_3$ suggested that not all of the methyl groups of vtmos condensed with the hydroxyl on ACF surface. Thus, the further condensation reaction of vtmos hardly took place on ACF surface in the process of hydrophobisation [26]. This probably explained why the pore did not altered drastically by the hydrophobisation (see Table 1).

According to the literature [25,26], the solid-state ^{29}Si NMR spectrum can give more direct evidence of the silicon functional groups grafted on the ACF surface. Fig. 4 gave the solid-state ^{29}Si NMR spectrum of ACF-H at 300 MHz. Depending on the spectrum, the peak at −80.89 ppm could be observed. Such chemical shift do not correspond to those (−53 ppm and −63 ppm) of the silicon present in the vtmos [39], thus confirming that vtmos is not adsorbed on ACF surface, but has reacted with it.

Fig. 3. FTIR spectra of ACF and ACF-H.

Table 1
Physical characteristic of ACF and ACF-H.

Samples	S_{BET} (m²/g)	Total pore volume V_{total} (cm³ g)	Micropore volume V_{micro} (cm³ g)	V_{total}/V_{micro} (%)	$D_{average}$ (nm)
ACF	1540.2	0.68	0.62	91.18	1.77
ACF-H	1336.5	0.58	0.54	93.10	1.74
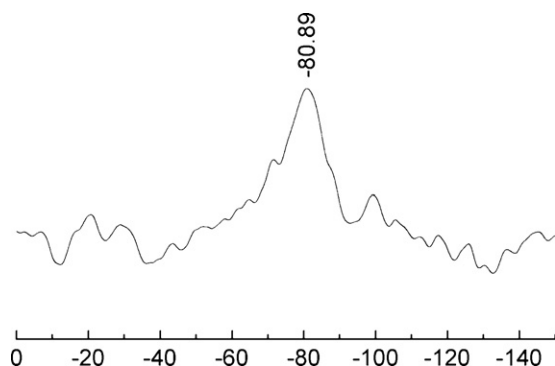
Fig. 4. ^{29}Si NMR spectrum of ACF-H.

In summary, the results illustrated by the FTIR spectroscopy and NMR spectra of ^{29}Si indicated that the organosilicon-containing groups existed on the surface of ACF. The condensation reaction between Si–O–CH$_3$ group and the –C–OH group had took place on the ACF surface, and then the –C–O–Si– group formed. These were consistent with the conclusions obtained by Budarin et al. and Cosnier et al. respectively [25,26].

3.2. Textural structure and thermal stability

It was found that the hydrophobisation of carbon surface altered the pore texture [26]. In order to study the effect of hydrophobisation on the pore texture, the nitrogen adsorption isotherms of samples was analyzed in this work.

Fig. 5 presents the nitrogen adsorption isotherms of ACF and ACF-H. It could be seen that both the two samples showed type I behavior according to the IUPAC classification [35], indicating a similar pore texture and pore size distribution (PSD) of ACF before and after the hydrophobisation. Such results showed that the hydrophobisation did not alter the pore texture drastically. On the other hand, the decrease of the nitrogen adsorption amount suggested the decrease in the BET surface and the pore volume induced by the hydrophobisation. The adsorption isotherms were analyzed by BJH method in order to further investigate the influence of hydrophobisation modification on the pore texture of ACF.
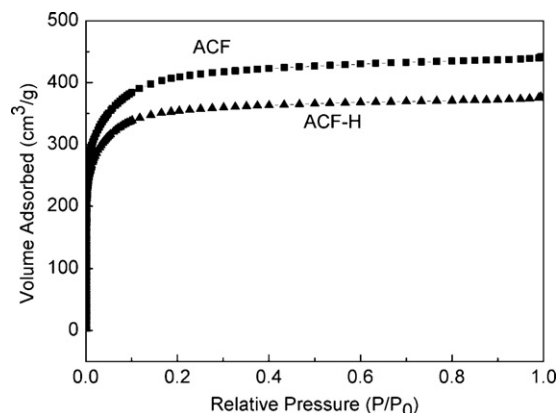
The results illustrated that the MPSD of ACF-H remained close to those of ACF (see Fig. 6). It could be observed that their relative proportions of the narrowest pores (<0.6 nm) and the pores larger than 3.2 nm remained almost unchanged. Only the pore volume relative proportions of micropores of ACF-H between 0.6 nm and 3.2 nm decreased slightly. These variations of the pore volume relative proportions were very likely related to the molecular dimension of vtmos (whose maximum molecular diameter was 0.73 nm). Due to the molecular dimension, the vtmos could not be grafted easily on the active sites around the pore-mouths with the pore width less than 0.6 nm; On the other hand, the grafting of vtmos could hardly influenced the pore width larger than 3.2 nm.

Table 1 showed the pore texture parameters of two samples. It was evident that the BET surface area, total pore volume, micropore volume and the mean pore width of ACF-H decreased slightly after hydrophobisation, which were consisted to the aforementioned findings illustrated by Figs. 3 and 4. These decreases of the pore texture parameters could be ascribed to vtmos grafting at the defect sites in the edges of the carbon layers and the pore-mouths [36]. Taking into consideration of the variations of the pore texture parameters, it was reasonable to suppose that the hydrophobisation modification was achieved by grafting the functional groups of vtmos onto the ACF surface rather than adsorbing on ACF. Moreover, the hydrophobisation did not alter the pore texture drastically. This was consistent with the results of Budarin et al. and Cosnier et al. [25,26].

The thermogravimetric data of ACF and ACF-H are given in Fig. 7. Comparing with the DTG curves of ACF, three new well-defined weight loss regions were observed in the DTG curve of ACF-H. The first weight loss region appeared in the region from 200 to 400 °C, the second from 400 °C to 700 °C, and the third from 700 °C to 800 °C. The first weight loss regions could be ascribed to the loss of three different kinds of methyl groups. According to the curve, there were three peaks in this weight loss region, which could be ascribed to the thermal decomposition of the different three methyl groups from vtmos. This indicated the three different kinds of methyl groups had their different bonding energies. The second weight loss region, with a sharp peak at 430 °C, could be attributed to the thermal decomposition of vtmos along with the evolution of CO$_2$, which originated from the thermal decomposition

Fig. 5. Nitrogen adsorption isotherms of ACF and ACF-H.
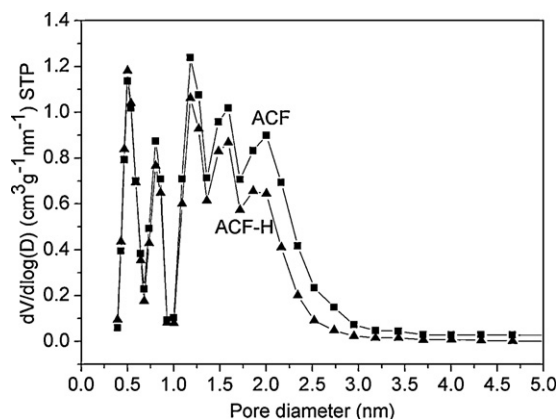
Fig. 6. MPSD of the ACF and ACF-H.
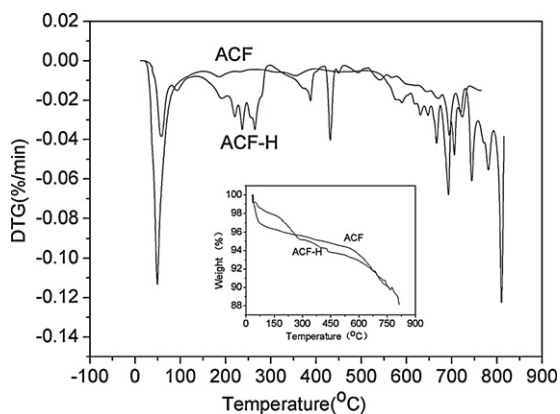
Fig. 7. Thermogravimetric analysis of ACF and hydrophobised ACF.

of the remaining unreacted organic groups of the grafted alkoxide [25,26]. The third weight loss peak could be assigned to the polymerisation of those grafted unsaturated functional groups, which was considered to be initiated by the reaction of radicals in those surface groups of the samples at high temperature (from 700 °C to 800 °C) [25].

The findings from thermogravimetric curve also indicated that the vtmos were grafted on the carbon surface. Concerning the high temperature (220 °C) of the weight loss regions, the hydrophobised ACF had a good thermal stability as an adsorbent in engineering application.

3.3. Wetting property

Besides the aforementioned characterizations, the wetting property test was introduced to investigate the efficiency of the hydrophobisation, which was tested by the small pieces with the length of 10 mm × 10 mm. The data of dynamic contact angle measurements of ACF and ACF-H are listed in Table 2. It was illustrated that the contact angle increased from 63.37° to 71.32°, suggesting the enhancement of the surface hydrophobicity of ACF-H.

The result of elemental analysis of the samples is listed in Table 2. The increase of the silicon content was observed and then the organosilicon groups enhanced the hydrophobicity. This gave the direct evidence of the enhancement of the surface hydrophobicity induced by the hydrophobisation.

3.4. Adsorption performance

At the present work, the static adsorption and dynamic adsorption experiments were conducted to evaluate the adsorption performance of the ACF after hydrophobisation, especially in high humidity.

As illustrated in Fig. 8(a), both the two samples showed type I behavior for CS_2 absorption, which was also observed from nitrogen adsorption isotherm, supporting the conclusion that the pore texture remained similar after hydrophobisation. The adsorption type of the two samples was micropore adsorption. The slight decrease of CS_2 adsorption capacity was found in the adsorption isotherm of ACF-H, ascribing to the slight reduction of BET surface area and
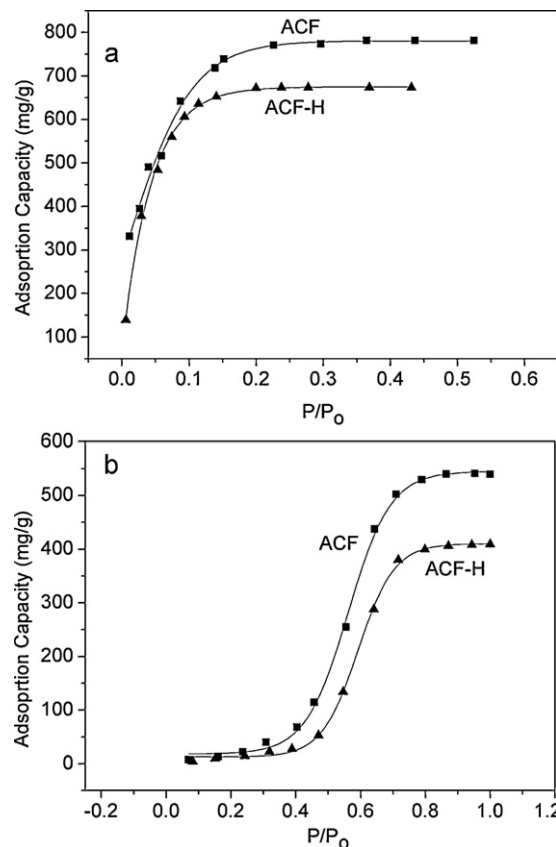
Fig. 8. Static adsorption isotherms of ACF and ACF-H, (a) CS_2 adsorption isotherms, (b) water adsorption isotherms.

micropore volume (shown in Table 1) induced by hydrophobisation. Even though the adsorption capacity had a slight decrease, ACF-H had remained a good adsorption performance in the process of static adsorption.

For water absorption, the type V adsorption isotherms over two materials were observed (see Fig. 8(b)). Comparing to the CS_2 adsorption, the difference should be relevant to the different adsorption driving force between adsorbate and adsorbent. The adsorption between the CS_2 and ACF was mainly due to the driving force of volume filling into micropores. In contrast, the adsorption between the water and ACF was much more complicated. The adsorption of water onto the ACF surface, which was promoted by acidic oxygen-containing groups of carbon surface as reported [40], might be mainly caused by the electrostatic interactions between water and the oxygen-containing groups on the ACF surface at low relative pressure. But at high P/P_0, it was more likely affected by pore texture [25]. These features led to the different adsorption behavior between water and CS_2. Another variation observed from Fig. 8(b) was the decrease of the water adsorption capacity on ACF, due to either the decrease of the BET surface area, pore volume or the enhancement of the hydrophobicity. Comparing to CS_2 adsorption, the decrease of the water adsorption amount was bigger than that of CS_2, especially in the range of relative pressure 0.3–0.7 (typically encountered in actual production). However, it was rather

Table 2
Wetting property and element analysis.

	Contact angle			Element analysis		
	Advancing angle (°)	Receding angle (°)	Contact angle (°)	C (%)	O (%)	Si (%)
ACF	65.83	60.91	63.37	91.07	7.29	0
ACF-H	75.09	67.54	71.32	88.42	7.27	3.27
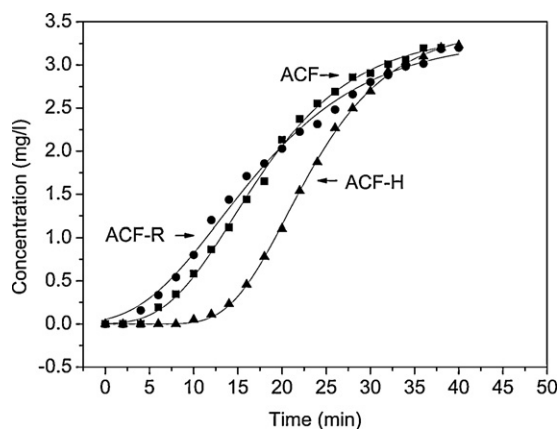
Fig. 9. Breakthrough curves of ACF, ACF-R and ACF-H.

difficult to verify clearly the effect of hydrophobisation on the water adsorption by static adsorption. Thus, in order to distinguish the nature of water adsorption on ACF, the dynamic adsorption evaluation was conducted under the humidity conditions.

The corresponding adsorption curves in Fig. 9 was obtained at a concentration of CS_2 of $C_o = 0.32\,mg\,l^{-1}$ with the relative humidity of 70%. The adsorption curve of ACF-R was presented here to demonstrate whether the pretreatment improved the adsorption performance under the humidity condition. The lengthening of adsorption time and the postponement of breakthrough time ($C/C_o = 0.1$) indicated that hydrophobic ACF had a better performance than ACF and ACF-R in the CS_2 adsorption process under the humidity condition at 70%.

Even though the aforementioned static adsorption experiment indicated that the hydrophobisation decreased the BET surface as well as the equilibrium adsorption capacity of CS_2 and water, the dynamic adsorption showed the contrary result that ACF-H had the better adsorption performance than ACF and ACF-R under the humidity condition at 70%. The pretreatment had not changed the adsorption performance of the material. These results demonstrated that the hydrophobisation indeed improved the adsorption selectivity toward CS_2.

As far as we know, there are many kinds of oxygen-containing groups on the surface of carbon-based materials, which led to both polar and hydrophilic properties [36]. Thus, polar molecular water would be easily adsorbed because of the affinity of water and oxygen-containing groups on the carbon surface [40,41]. Moreover, water adsorbed on carbon surface could form water clusters [42–44], and those water clusters in a 3D configuration could block the pores through which CS_2 molecules passed into micropores [40]. On the other hand, for the nonpolar molecular CS_2, the interactions between CS_2 and the oxygen-containing groups on the ACF surface were principally unfavourable. In a word, the increase of the adsorption selectivity toward CS_2 could be attributed to the improvement of the hydrophobicity induced by grafting of organosilicon groups. The nonpolar methoxyl groups of vtmos decreased the adsorption of water and thus reduced the water clusters. Consequently, the negative influence of water on the adsorption of CS_2 was limited by the hydrophobisation which resulted in the increase of the adsorption selectivity toward CS_2.

4. Conclusions

The surface hydrophobisation of the viscose-based commercial ACF was carried out by grafting vinyltrimethoxysilane (vtmos) onto the surface of ACF, which pretreated by H_2O_2 and $NaBH_4$. The characterizations indicated that the organosilicon group from

vtmos was grafted onto the surface of the ACF. Simultaneously, the static and dynamic adsorption was carried out to illustrate the hydrophobisation effect. Even though both CS_2 and water equilibrium adsorption capacity slightly decreased due to the variations of pore texture induced by the hydrophobisation, the adsorption selectivity toward CS_2 was indeed enhanced under the humidity condition at 70%, which could be attributed to the enhancement of the surface hydrophobicity. The hydrophobisation declined the interactions between water molecular and the oxygen-containing groups on the AC surface. As a result, such a modification evidently improved the hydrophobicity and then their selective adsorption towards CS_2 of ACF under the highly humid condition.

References

[1] W. Hugler, C. Acosta, S. Revah, Environ. Prog. 18 (1999) 173.
[2] J. Yang, P. Juan, Z.M. Shen, R. Guo, J.P. Jia, H.J. Fang, Y.L. Wang, Carbon 44 (2006) 1367.
[3] Y. Yegiazarov, J. Clark, L. Potapova, V. Radkevich, V. Yatsimirsky, D. Brunel, Catal. Today 102–103 (2005) 242.
[4] E.F. Spink, K.R. Muller, Removal of contaminations from gas streams of viscose fiber manufacture, Pat. RF No. 2199376C2, 2003, ICI 7B01D 53/52.
[5] T. Morooka et al., Method of CS_2 removal, Pat. Jap. No. 3265589B2, 2002, ICI 7B01D 53/86.
[6] H.J. Fang, H.Q. Hou, L.Y. Xia, X.H. Shu, R.X. Zhang, Chemosphere 69 (2007) 1734.
[7] N.A. Smith, D.P. Kelly, J. Gen. Microbiol. 134 (1988) 3041.
[8] D. Scarano, S. Bertarione, A. Zecchina, R. Soave, G. Pacchioni, Phys. Chem. Chem. Phys. 4 (2002) 366.
[9] B. Guo, L.P. Chang, K.C. Xie, Fuel Process. Technol. 87 (2006) 873.
[10] X. Huang, B.J. Li, G.W. Gu, Ion Exch. Adsorpt. 7 (1991) 195.
[11] X. Huang, B.J. Li, G.W. Gu, Ion Exch. Adsorpt 8 (1992) 15.
[12] Z.Y. Xie, J.P. Li, N. Zhao, F. Wang, W.C. Peng, F.K. Xiao, W. Wei, Y.H. Sun, New Carbon Mater. 24 (2009) 260.
[13] D. Das, V. Gaur, N. Verma, Carbon 42 (2004) 2949.
[14] P. Navarri, D. Marchal, A. Ginestet, Filtr. Sep. 33 (2001) 34.
[15] P.D. Sullivan, M.J. Rood, Environ. Sci. Technol. 38 (2004) 4865.
[16] J.H. Tsai, H.M. Chiang, G.Y. Huang, H.L. Chiang, J. Hazard. Mater. 54 (2008) 1183.
[17] P. Dwivedi, V. Gaur, A. Sharma, N. Verma, Sep. Purif. Technol. 39 (2004) 23.
[18] M. Suzuki, Carbon 321 (1994) 577.
[19] X.H. Shao, W.C. Wang, X.J. Zhang, Carbon 45 (2007) 188.
[20] M.H. Manero, R.K. Jain, Y. Aurelle, C. Cabassud, M. Roustan, in: S.P. Shelton (Ed.), Environmental Technologies and Trends, Springer, New York, 1996, p. 87.
[21] H.L. Fan, C.H. Li, H.X. Guo, J. Nat. Gas Chem. 8 (1999) 151.
[22] J.K. Brennan, T.J. Bandosz, K.T. Thomson, K.E. Gubbins, Colloid Surf. A 187–188 (2001) 539.
[23] J.A. Menéndez, B. Xia, J. Phillips, L.R. Radovic, Langmuir 13 (1997) 3414.
[24] A. Arenillas, F. Rubiera, J.B. Parra, C.O. Ania, J.J. Pis, Appl. Surf. Sci. 252 (2005) 619.
[25] V.L. Budarin, J.H. Clark, S.V. Mikhalovsky, A.A. Gorlova, N.A. Boldyreva, V.K. Yatsimirsky, Adsorpt. Sci. Technol. 18 (2000) 55.
[26] F. Cosnier, A. Celzard, G. Furdin, D. Bégin, J.F. Marêché, O. Barrès, Carbon 43 (2005) 2554.
[27] Y. Nakanishi, K. Honjo, T. Honjo, Surface-hydrophobic activated carbon and its manufacture, Pat. EP No. 0765840A1, 1997, ICI C01B 31/08.
[28] T.A. Ryan, H. Sharrock, Activated carbon treated with siliconcontaining compounds, Pat. GB No. 2391224A, 2004, ICI C01B 31/08.
[29] S.S. Barton, M.J.B. Evans, S. Liang, J.A.F. Macdonald, Carbon 34 (1996) 975.
[30] M.R. Wertheimer, J.E. Klemberg-Sapieha, J. Cerny, S. Liang, Plasma Polym. 3 (1998) 151.
[31] P.J.M. Carrott, J.M.V. Nabais, M.M.L. Ribeiro Carrott, J.A. Menéndez, Microporous Mesoporous Mater. 47 (2001) 243.
[32] J.M. Valente Nabais, P.J.M. Carrott, M.M.L. Ribeiro Carrott, J.A. Menéndez, Carbon 42 (2004) 1315.
[33] H.C. Huang, D.Q. Ye, B.C. Huang, Surf. Coat. Technol. 201 (2007) 9533.
[34] D.F. Zhang, W. Lu, P.P. Wang, L.L. Yang, C.X. Li, X.D. Ceng, J. China Coal Soc. 33 (2008) 439.
[35] M. Suzuki, Adsorption Engineering, Elsevier, Amsterdam, 1990, p86.
[36] H.P. Boehm, Carbon 32 (1994) 759.

[37] K. Semba, H. Morita, J. Photochem. Photobiol. A: Chem. 146 (2001) 141.
[38] SDBS (Integrated Spectral Data Base System for Organic Compounds) databank, web page: http://www.aist.go.jp/RIODB/SDBS/.
[39] M.C. Douskey, M.S. Gebhard, A.V. McCormick, B.C. Lange, D.W. Whitman, Prog. Org. Coat. 45 (2002) 145.
[40] B. Li, Z. Lei, Z. Huang, Chem. Eng. Technol. 32 (2009) 763.
[41] F.P. Villacañas, M.F.R. José, J.M. Órfão, J.L. Figueiredo, J. Colloid Interface Sci. 293 (2006) 128.
[42] O.P. Mahajan, C. Moreno-castilla, P.L. Walker, Sep. Sci. Technol. 15 (1980) 1733.
[43] M. Franz, H.A. Arafat, N.G. Pinto, Carbon 38 (2000) 1807.
[44] A. Dąbrowski, P. Podkościelny, Z. Hubicki, M. Barczak, Chemosphere 58 (2005) 1049.